DOI 10.2478/ama-2024-0058

ANALYTICAL ANALYSIS OF THERMAL CONDUCTIVITY BY LAMINAR FLOW UNDER THE INFLUENCE OF MHD USING VOGEL'S MODEL

Rashid NAWAZ*/, Muhammad FAROOQ***
Siddiq Ur REHMAN*, Gamal M. ISMAIL*, Hijaz AHMAD***/****/*****/******

*Department of Mathematics, Abdul Wali Khan University, Mardan, Khyber Pakhtunkhwa, Pakistan
**UniSa STEM, University of South Australia, Australia
***Department of Mathematics, Faculty of Science, Islamic University of Madinah, Madinah, 42351, Saudi Arabia
****Near East University, Operational Research Center in Healthcare, TRNC Mersin 10, Nicosia, 99138, Turkey
*****Department of Computer Science and Mathematics, Lebanese American University, Beirut, Lebanon
******Department of Mathematics and Informatics, Azerbaijan University, Jeyhun Hajibeyli street, 71, AZ1007, Baku, Azerbaijan

rashidnawaz@awkum.edu.pk, muhammadfarooq@awkum.edu.pk,
siddiqurrehman@awkum.edu.pk, gamalm2010@yahoo.com, hijaz555@gmail.com

received 16 July 2023, revised 26 August 2023, accepted 4 September 2023

Abstract: The main aim of this work is to study the influence of thermal conductivity of uniform couple stress fluid of inclined Poiseuille flow in the presence of magneto hydrodynamic (MHD) between two parallel plates. A well-known Vogel's viscosity model is used. The momentum and energy equations are solved analytically by utilizing Homotopy Perturbation method (HPM) and Optimal Homotopy Asymptotic Method (OHAM). The results include the velocity profile, average velocity, volume flux, Shear Stress, Skin friction and the temperature distribution between the plates. Particular attention is given to the effect of MHD Γ on the velocity field and temperature distribution. As can be seen, that there exists direct relation between MHD parameter Γ and velocity profile and bears inverse relation with temperature distribution. In addition to that, influence of non-dimensional parameters like G, A, a, B and γ on the velocity field and temperature distribution are also discussed graphically. The physical characteristics of the problem have been well discussed in graphs for several parameters of interest. The results reveal that both techniques are reliable and are in great agreement with each other.

Keywords: OHAM, HPM, Couple Stress Fluid, Magnetohydrodynamics, Vogel's Model

1. INTRODUCTION

In recent years, the flow of non-Newtonian fluids has attracted a great deal of interest due to the expanding industrial, medical, and technological applications. Numerous researchers have investigated certain flow issues with non-Newtonian fluids, such as couple stress fluid. Stokes's [1] theory of couple stress fluids has several medical, industrial, and scientific applications, including as the modelling of synthetic fluids, polymer thickened oils, liquid crystals, animal blood, and synovial fluid. The book by Stokes [2] covers some of the earliest developments in coupled stress fluid theory and basic flows. A few scholars have recently investigated some couple stress fluid flows for various flow geometries [3]-[8].

There are a number of suggested constitutive equations for non-Newtonian fluids, each of which attempts to provide an explanation for their behavior. Couple stresses, a non-symmetric stress tensor, and body couples are only a few of the unique characteristics of Stokes' couple stress fluid model. Models for fluids with mechanically important microstructures are proposed in Stokes' couple stress fluid theory. Microstructure can affect a liquid if the distinctive geometric dimension of the problem is on the same scale as the microstructure's size [9]. The introduction of a size-dependent effect is one of the major aspects of couple stresses. Classical continuum mechanics disregards the influence of material particle size inside the continuum. It is compatible with the symmetry of the force-stress tensor to disregard the rotational interaction between fluid particles. Clearly, this is not the case, and a size-dependent couple-stress theory is necessary in situations such as fluid flow with suspended particles when it must be used. The couple-stress tension caused by the microrotation of these freely floating particles led to the formation of couple-stress fluid. As shown by the couplet stress fluid, fluids may be used to describe a variety of lubricants, suspension fluids, blood, etc. These fluids are employed in a range of industrial processes, including liquid crystal solidification, polymer fluid extrusion, colloidal solutions, and the cooling of metallic plates in a bath.

A number of technological processes rely on heat transmission. Non-Newtonian mixtures require heat transfer for processing and management [10]. Mathematicians, engineers, and scientists find it hard to understand how nonlinear fluid flows work because the nonlinearity can show up in different ways. For example, studying reactive variable viscosity flows in a slit with wall injection or suction is a good example. In our case, the fact that viscosity changes with temperature is one of the reasons why the coupled ordinary differential equations are not linear. Different researchers look into flows with viscosity that changes with temperature [11]-[14]. Moreover, several scientists examined the effect of MHD on squeezing fluid flow through porous medium in [15]-[20]. Furthermore, the effect of MHD on micropolar fluid were analyzed by researchers in [21]-[24].

Many numerical, semi-numerical, analytical, and homotopy based strategies have been presented by mathematicians to solve nonlinear differential equations and related systems. The Optimal Homotopy Asymptotic Method (OHAM), which is used to solve differential equations, is one of the efficient homotopy based techniques. This technique was presented by Marinca et al. to solve differential equations. This perturbation approach works without small or big parameters, unlike other perturbation methods, and it does not require discretization, which requires time. Unlike iterative approaches, the procedure does not require a preliminary guess. The method's convergence is also changed by using a more variable function called the auxiliary function. One of OHAM's shortcomings is that the unknown auxiliary parameters which control the convergence are determined using the least squares approach, which requires extra time when dealing with highly nonlinear problem. The collocation approach is an alternative technique; however, accuracy would be compromised in the latter situation. Numerous issues have been resolved using this approach. When dealing with heat flux conditions, researchers converted highly nonlinear partial differential equations (PDEs) [25] [26] into structured ordinary differential equations (ODEs) with appropriate restrictions (OHAM). Recently, scientists and engineers have increased their usage of the Homotopy perturbation technique (HPM) [27] in nonlinear problems due to the fact that this method converts the tough problem under inquiry into a clear, easily-solvable problem. He invented and modified the homotopy perturbation method. after initially proposing [28] it in 1998. In the majority of instances, the approach results in a fairly quick convergence of the solution series. After only one iteration, the outcome is often quite accurate. By combining linear and nonlinear problems, He' s homotopy perturbation approach was created to solve beginning and boundary value problems. Most perturbation methods assume the presence of a tiny parameter, yet the vast majority of nonlinear problems lack any type of small parameter. Scientists have just begun to use homotopy perturbation theory, which, when properly combined with perturbation theory, has [29] [30] the potential to be a very effective mathematical tool. El-Shahed [31] recently used Volterra's integro differential equations to apply He's homotopy perturbation approach.

Keeping in mind the above literature survey, there is no analysis about the steady inclined Poiseuille flow under the influence of magneto hydrodynamic (MHD) between two parallel plates. Prior to computing the analytical results, the regulating flow expression is converted to an ordinary system. The two reliable analytical techniques OHAM and HPM are used to solve the governing system of couple equations. Velocity profile and temperature distribution are calculated numerically and graphically presented. The effect of various parameters i.e. G, A,Γ, γ and a are also discussed.

2. CHAPTER TITLE

Consider a fluid that is viscous, incompressible, and electrically conducts as it moves between two infinitely parallel inclined plates at the positions of y = −H (lower plate) and y = H (upper plate) under the influence of a persistent pressure gradient in the direction of motion and a steady transverse magnetic field Γ. The fluid still flows even while the plates are still. Temperatures of Θ_0 and Θ_1 are maintained for the bottom and top plates, respectively.

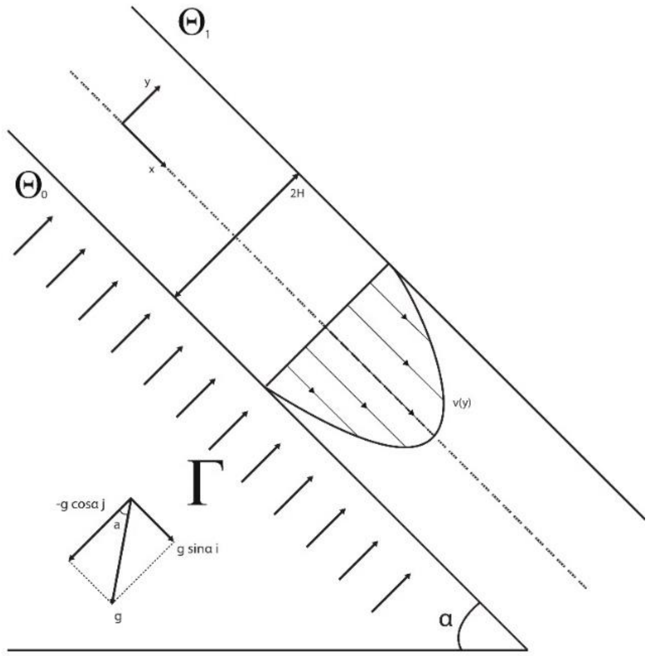

Fig 1. Geometry of the problem

Fig. (1) depicts the coordinate system that was chosen. The angle of the plate with regard to the horizontal direction is α. The viscosity η of a fluid is stated to be dependent on Θ. Velocity and temperature field are of the form:

$$\Upsilon = \Upsilon(v, 0,0), v = v(y), \Theta = \Theta(y), \tag{1}$$

The continuity equation [32]

$$\frac{\partial \rho}{\partial t} + \nabla \cdot (\rho \Upsilon) = 0, \tag{2}$$

is identically satisfied after applying assumptions (1). The three components of the momentum equation [32]

$$\rho \frac{D\Upsilon}{Dt} = \nabla \cdot T - \eta \nabla^4 \Upsilon + J \times B + \rho g, \tag{3}$$

become

$$0 = -\frac{\partial p}{\partial x} + \frac{\partial}{\partial x}(S_{xx}) + \frac{\partial}{\partial y}(S_{xy}) + \frac{\partial}{\partial z}(S_{xz}) - \eta \frac{d^4 v}{dy^4} - \sigma B_0 v + \rho g sin(\alpha), \tag{4}$$

$$0 = -\frac{\partial p}{\partial y} + \frac{\partial}{\partial x}(S_{yx}) + \frac{\partial}{\partial y}(S_{yy}) + \frac{\partial}{\partial z}(S_{yz}) - \rho g cos(\alpha), \tag{5}$$

$$0 = -\frac{\partial p}{\partial z} + \frac{\partial}{\partial x}(S_{zx}) + \frac{\partial}{\partial y}(S_{zy}) + \frac{\partial}{\partial z}(S_{zz}), \tag{6}$$

where B_0 denotes the applied magnetic field and σ denotes the fluid's electric conductivity, we know that

$$S_{xx} = S_{yy} = S_{zz} = S_{xz} = S_{zx} = S_{yz} = S_{zy} = 0, S_{xy} = \mu \frac{dv}{dy} = S_{yx}, \tag{7}$$

the following equations are derived by inserting these values into (4-6)

$$0 = -\frac{\partial p}{\partial x} + \frac{d}{dy}\left(\mu \frac{dv}{dy}\right) - \eta\, (d^4 v)/(dy^4) - \sigma \beta_0 v + \rho g sin(\alpha), \tag{8}$$

$$0 = -\frac{\partial p}{\partial y} - \rho g cos(\alpha), \tag{9}$$

DOI 10.2478/ama-2024-0058

$$0 = -\frac{\partial p}{\partial z}, \tag{10}$$

The velocity profile is obtained from (4). This equation may also be expressed as

$$\eta \frac{d^4 v}{dy^4} - \mu \frac{d^2 v}{dy^2} - \frac{d\mu}{dy}\frac{dv}{dy} + \frac{\partial p}{\partial x} + \sigma\beta_0 v - \rho g \sin(\alpha) = 0. \tag{11}$$

After applying all presumptions, the energy equation [32]

$$\rho c_p \frac{D\Theta}{Dt} = \kappa \nabla^2 \Theta + tr(T \cdot L), \tag{12}$$

simplifies to the Eq. (13)

$$\frac{d^2 \Theta}{dy^2} + \frac{\mu}{\kappa}\left(\frac{dv}{dy}\right)^2 + \frac{\mu}{\kappa}\left(\frac{d^2 v}{dy^2}\right)^2 = 0, \tag{13}$$

The corresponding boundary conditions are

$$v(y = \pm H) = 0, \tag{14}$$

$$\frac{d^2}{dy^2} v(y = \pm H) = 0, \tag{15}$$

$$\Theta(y = -H) = \Theta_0, \Theta(y = H) = \Theta_1. \tag{16}$$

The standard no-slip boundary conditions are given in Eq. (14). According to Eq. (15), couple stresses at the plates are zero. The following non-dimensional parameters are introduced [32]:

$$v^{\cdot} = \frac{v}{V}, y^{\cdot} = \frac{y}{H}, x^{\cdot} = \frac{x}{H}, \Theta^{\cdot} = \frac{\Theta - \Theta_0}{\Theta_1 - \Theta_0}, \mu^{\cdot} = \frac{\mu}{\mu_0}, p^{\cdot} = \frac{p}{\mu_0 \frac{V}{H}},$$

$$\gamma = \frac{\mu_0 V^2}{\kappa(\Theta_1 - \Theta_0)}, B^2 = \frac{\mu_0(H^2)}{\eta}, G = -\frac{B^2 H^5}{\mu_0 V}\frac{\partial p}{\partial x}, A = \frac{\rho g H^4}{\eta V}.$$

Hence Γ in terms of parameters are as follows $\Gamma = \frac{\sigma B_0^2 H^4}{\eta}$. Where γ is the Brinkman number, μ Is the reference viscosity, and V is the reference velocity. Using these dimensionless parameters, equation (11) and (13) along with the boundary conditions becomes (dropping dots)

$$\frac{d^4 v}{dy^4} - B^2 \mu \frac{d^2 v}{dy^2} - B^2 M \frac{d\mu}{dy}\frac{dv}{dy} + \Gamma v + A \sin(\alpha) - G = 0, v(y = \pm 1) = \frac{d^2}{dy^2} v(y = \pm 1) = 0, \tag{17}$$

$$\frac{d^2 \Theta}{dy^2} + \gamma\mu\left(\frac{dv}{dy}\right)^2 + \frac{\gamma}{B^2}\left(\frac{d^2 v}{dy^2}\right)^2 = 0, \Theta(y = -1) = 0, \Theta(y = 1) = 1. \tag{18}$$

The following is an expression for the dimensionless form of the Vogel's viscosity model [33]:

$$\mu = \mu_* \exp\left(\frac{A_0}{B_0 + \Theta} - \Theta_w\right). \tag{19}$$

Using Taylor series expansion on Eq. (19) we get

$$\mu = a^2 \left(1 - \frac{A_0 \Theta}{B_0^2}\right). \tag{20}$$

Assume that $M = A_0/(B_0^2)$, then (20) becomes

$$\mu = a^2 (1 - M\Theta), \frac{d\mu}{dy} = -a^2 M \frac{d\Theta}{dy}. \tag{21}$$

The coupled system shown below is generated by substituting Eq. (20) in the governing Eqs. (17) and (18):

$$\frac{d^4 v}{dy^4} - B^2 a^2 (1 - M\Theta)\frac{d^2 v}{dy^2} + B^2 M a^2 \frac{d\Theta}{dy}\frac{dv}{dy} + \Gamma v + A \sin(\alpha) - G = 0, v(y = \pm 1) = \frac{d^2}{dy^2} v(y = \pm 1) = 0, \tag{22}$$

$$\frac{d^2 \Theta}{dy^2} + \gamma a^2 (1 - M\Theta)\left(\frac{dv}{dy}\right)^2 + \frac{\gamma}{B^2}\left(\frac{d^2 v}{dy^2}\right)^2 = 0, \Theta(y = -1) = 0, \Theta(y = 1) = 1. \tag{23}$$

3. BASIC NOTION OF METHODS

3.1. Fundamental concept of OHAM

Let us examine a boundary value problem, as well as the boundary conditions

$$\chi[X(y)] + g(y) + \xi[X(y)] = 0, \tag{24}$$

$$\beta(X, \frac{\partial X}{\partial y}) = 0. \tag{25}$$

In this notation, y is the dependent variable, $X(y)$ is the unknown function, $g(y)$ is the known function, χ, ξ and β are the linear, nonlinear, and boundary operators, respectively.

The OHAM states that the homotopy $\hbar(G(y,\rho),\rho): R \times [0,1] \to R$ satisfies

$$(1-\rho)[\chi(G(y,\rho)) + g(y)] = \hbar(\rho)[\chi(G(y,\rho)) + g(y) + \xi(G(y,\rho))], \tag{26}$$

$$\beta\left(G(y,\rho), \frac{\partial G(y,\rho)}{\partial y}\right) = 0,$$

for $y \in R$ and $\rho \in [0,1]$, is generated using the non-zero auxiliary function $\hbar(\rho)$ for $\rho \neq 0$ with $\hbar(0) = 0$ and a function $G(y,\rho)$ whose value is unknown. $G(y,0) = X_0(y)$ and $G(y,1) = X(y)$ remain true when $\rho = 0$ and 1. Hence, as ρ varies from 0 to 1, the solution $G(y,\rho)$ changes from $X_0(y)$ to $X(y)$.
for $\rho = 0$,

$$\chi[X_0(y)] + g(y) = 0, \beta\left(X_0(y), \frac{dX_0(y)}{dy}\right) = 0. \tag{27}$$

We pick the auxiliary function $\hbar(\rho)$ in such a manner that

$$\hbar(\rho) = \sum_{i=0}^{n} \rho^i C_i, \tag{28}$$

where C_i are the constants governing convergence that must be calculated. Expanding Taylor's series $G(y,\rho)$ about ρ to obtain an approximation

$$G(y,\rho,C_i) = X_0(y) + \sum_{j=1}^{n} X_j(y, C_1, C_2, \ldots, C_j)\rho^j. \tag{29}$$

Equating the coefficients of identical powers of ρ by putting (29) into (26) provides the following findings.
for $\rho = 1$,

$$\chi[X_1(y)] + g(y) = C_1 \xi_0 [X(y)], \beta\left(X_1(y), \frac{dX_1(y)}{dy}\right) = 0. \tag{30}$$

for $\rho = 2$,

$$\chi[X_2(y)] - \chi[X_1(y)] = C_2 \xi_0 [X_0(y)] + C_1 \left[\chi(X_1(y)) + \xi_1(X_0(y), X_1(y))\right], \beta\left(X_2(y), \frac{(dX_2(y))}{dy}\right) = 0. \tag{31}$$

generally

$\chi[X_n(y)] - \chi[X_{n-1}(y)] =$
$C_n \xi_0 [X_0(y)] +$
$\left(\sum_{j=1}^{n-1}\left[\chi[X_{n-j}(y)] + \xi_{n-j}(X_0(y), X_1(y), \cdots, X_{n-1}(y))\right]\right),$ (32)

with boundary conditions

$$\beta\left(X_k(y), \frac{dX_k(y)}{dy}\right) = 0, k = 2,3,4 \ldots \quad (33)$$

Where $\xi_m(X_0(y), X_1(y), \cdots, X_{m-1}(y))$ is the coefficient of ρ^m in the expansion of $\xi(G(y,\rho))$ about ρ as

$$\xi(G(y,\rho,C_i)) = \xi_0[X_0(y)] + \sum_{m=1}^{\infty} \xi_m(X_0(y), X_1(y), \cdots, X_{m-1}(y))\, \rho^m \quad (34)$$

The convergence of the series (29) is determined by C_i. For convergence at $\rho = 1$, the rth-order approximation $\cancel{G}$ is

$$\cancel{G}(y, C_1, C_2, \cdots, C_r) = X_0(y) + \sum_{j=1}^{r} X_j(y, C_1, C_2, \cdots, C_j). \quad (35)$$

Placing (35) in (24) the expression for the residual is

$$R(z, C_1, C_2, \cdots, C_r) = \chi[\cancel{G}(y, C_1, C_2, \cdots, C_r)] + g(y) + \xi[\cancel{G}(y, C_1, C_2, \cdots, C_r)]. \quad (36)$$

If $R = 0$, $\cancel{G}$ will be the exact solution, however this is typically not the case in nonlinear situations. There are numerous approaches for determining the optimal values of the constants C_i. Following is the application of the least-squares approach.

$$J = \int_a^b R^2(z, C_1, C_2, \cdots, C_r)dz. \quad (37)$$

Minimizing this function, we have

$$\frac{\partial J}{\partial C_i}(y, C_1, C_2, \cdots, C_r) = 0, i = 1,2,3, \cdots, r. \quad (38)$$

Where a and b are chosen from the problem's domain in order to locate C_i. For these values of C_i, the approximation solution is well-defined.

3.2. Fundamental concept of HPM

Take the following nonlinear differential equation to illustrate the operation of HPM:

$$\Xi[X(y)] + g(r) = 0, r \in \Omega, \quad (39)$$

with the boundary conditions

$$\beta\left(X(y), \frac{\partial X(y)}{\partial y}\right) = 0, r \in \Lambda. \quad (40)$$

Ξ is a basic differential operator, β is a boundary operator, $g(r)$ is a well-known analytic function, and Λ is the domain boundary for Ω.

The operator Ξ is decomposed into two pieces, χ and ξ, where χ is linear and ξ is nonlinear. Hence, Eq. (39) may be expressed as follows:

$$\chi[X(y)] + \xi[X(y)] - g(r) = 0, \quad (41)$$

He [9] built a homotopy $\chi : \Omega \times [0,1] \rightarrow R$ that meets the condition,

$$H(X,\rho) = (1-\rho)[\chi(X) - \chi(X\_0)] + \rho[\Xi(X) - g(r)] \quad (42)$$

or

$$H(X,\rho) = \chi(X) - \chi(X_0) + \rho[\chi(X_0)] + \rho[\xi(X) - g(r)]. \quad (43)$$

Where $r \in \Omega, \rho \in [0,1]$ which is referred to as the homotopy parameter, and X_0 is the initial approximation of the function (39). Hence, it concludes that

$$H(X,0) = \chi(X) - \chi(X_0) = 0, H(X,1) = \Xi(X) - g(r) = 0, \quad (44)$$

and the procedure of moving ρ from 0 to 1 is identical to that of $H(X,\rho)$ from $\chi(X) - \chi(X_0)$ to $\Xi(X) - g(r)$. This is known as deformation in topology, $\chi(X) - \chi(X_0)$ and $\Xi(X) - g(r)$ are called homotopic. Using the perturbation approach [10], and assuming that $0 \leq \rho \leq 1$ is a small parameter, we may suppose that the solution of (42) or (43) can be written as a series in ρ, as shown below

$$X = X_0 + \rho X_1 + \rho^2 X_2 + \rho^3 X_3 + \cdots \quad (45)$$

when ρ → 1, (42) or (43) corresponds to (41) and becomes the approximate solution of (41), i.e.

$$X(y) = \lim_{\rho\to 1} X = X_0 + X_1 + X_2 + X_3 + \ldots \quad (46)$$

The convergence rate of the series (46) is dependent on $\Xi(X)$ [11] in the majority of situations.

4. SOLUTIONS OF THE PROBLEM

4.1. OHAM solution

Zero component of velocity and temperature distribution along with the boundary conditions are given by

$$\frac{d^4}{dy^4} v_0(y) + A\sin(\alpha) - G = 0, \quad (47)$$

$$v_0(y = \pm 1) = 0, \frac{d^2}{dy^2} v_0(y = \pm 1) = 0,$$

$$\frac{d^2}{dy^2}\Theta_0(y) = 0, \quad (48)$$

$$\Theta_0(y = -1) = 0, \Theta_0(y = 1) = 1.$$

Their solutions are

$$v_0(y) = \frac{1}{24}(5G - 6Gy^2 + Gy^4 - 5A\sin(\alpha) + 6Ay^2\sin(\alpha) - Ay^4\sin(\alpha)), \quad (49)$$

$$\Theta_0(y) = \frac{1+y}{2}. \quad (50)$$

First component of velocity and temperature distribution along with the boundary conditions are given by

$$-a^2 B^2 c_1 M \frac{d}{dy} v_0(y) \frac{d}{dy}\Theta_0(y) - a^2 B^2 c_1 M\Theta_0(y) \frac{d^2}{dy^2} v_0(y) + a^2 B^2 c_1 \frac{d^2}{dy^2} v_0(y) - A\sin(\alpha) - Ac_1\sin(\alpha) + c_1 G - c_1 \Gamma v_0(y) - c_1 \frac{d^4}{dy^4} v_0(y) + G - \frac{d^4}{dy^4} v_0(y) + \frac{d^4}{dy^4} v_1(y) = 0, \quad (51)$$

$$v_1(y = \pm 1) = 0, \frac{d^2}{dy^2} v_1(y = \pm 1) = 0.$$

DOI 10.2478/ama-2024-0058

$$-a^2\gamma c_4\left(\frac{d}{dy}v_0(y)\right)^2+a^2M\gamma c_4\Theta_0(y)\left(\frac{d}{dy}v_0(y)\right)^2-\frac{1}{B^2}\gamma c_4\left(\frac{d^2}{dy^2}v_0(y)\right)^2-\frac{d^2}{dy^2}\Theta_0(y)-c_4\frac{d^2}{dy^2}\Theta_0(y)+\frac{d^2}{dy^2}\Theta_1(y)=0, \quad (52)$$

$$\Theta_1(y=-1)=0,\Theta_1(y=1)=0.$$

Their solutions are

$$v_1(y)=\frac{1}{40320}(c_1(y^2-1)(G-A\sin(\alpha))(4a^2B^2(M(y(y(y(y(4y+7)-38)-98)+74)+427)-14(y^4-14y^2+61))+\Gamma(y^6-27y^4+323y^2-1385))), \quad (53)$$

$$\Theta_1(y)=-\frac{1}{181440B^2}\left(\gamma c_4(y^2-1)\left(a^2B^2\left(35My^7+45(M-2)y^6-325My^5-459(M-2)y^4+809My^3+1431(M-2)y^2+809My+1431(M-2)\right)-1512(y^4-4y^2+11)\right)(G-A\sin(\alpha))^2\right), \quad (54)$$

Second component of velocity and temperature distribution along with the boundary conditions are given by

$$Gc_2-A\sin(\alpha)c_2-\Gamma c_2v_0(y)-\Gamma c_1v_1(y)-a^2B^2Mc_2\frac{d}{dy}v_0(y)\frac{d}{dy}\Theta_0(y)-a^2B^2Mc_1\frac{d}{dy}v_1(y)\frac{d}{dy}\Theta_0(y)-a^2B^2Mc_1\frac{d}{dy}v_0(y)\frac{d}{dy}\Theta_1(y)+a^2B^2c_2\frac{d^2}{dy^2}v_0(y)-a^2B^2c_2\Theta_0(y)\frac{d^2}{dy^2}v_0(y)-a^2B^2Mc_1\Theta_1(y)\frac{d^2}{dy^2}v_0(y)+a^2B^2c_1\frac{d^2}{dy^2}v_1(y)-a^2B^2Mc_1\Theta_0(y)\frac{d^2}{dy^2}v_1(y)-c_2\frac{d^4}{dy^4}v_0(y)-\frac{d^4}{dy^4}v_1(y)-c_1\frac{d^4}{dy^4}v_1(y)+\frac{d^4}{dy^4}v_2(y)=0, \quad (55)$$

$$v_2(y=\pm1)=0,\frac{d^2}{dy^2}v_2(y=\pm1)=0,$$

$$-a^2\gamma c_5\left(\frac{d}{dy}v_0(y)\right)^2+a^2M\gamma c_5\Theta_0(y)\left(\frac{d}{dy}v_0(y)\right)^2+a^2M\gamma c_4\Theta_1(y)\left(\frac{d}{dy}v_0(y)\right)^2-2a^2c_4\gamma\frac{d}{dy}v_0(y)\frac{d}{dy}v_1(y)+2a^2M\gamma c_4\Theta_0(y)\frac{d}{dy}v_0(y)\frac{d}{dy}v_1(y)-\frac{1}{B^2}\gamma c_5\left(\frac{d^2}{dy^2}v_0(y)\right)^2-\frac{1}{B^2}2\gamma c_4\frac{d^2}{dy^2}v_0(y)\frac{d^2}{dy^2}v_1(y)-c_5\frac{d^2}{dy^2}\Theta_0(y)-\frac{d^2}{dy^2}\Theta_1(y)-c_4\frac{d^2}{dy^2}\Theta_1(y)+\frac{d^2}{dy^2}\Theta_1(y)=0, \quad (56)$$

$$\Theta_2(y=-1)=0,\Theta_2(y=1)=0.$$

Their solutions are

$$v_2(y)=-\frac{1}{261534873600}(y^2-1)(G-A\sin(\alpha))(c_1(2a^2\gamma c_4M\left(a^2B^2\left(1540My^{13}+2475(M-2)y^{12}-31010My^{11}-55674(M-2)y^{10}+237622My^9+511893(M-2)y^8-573188My^7-1515132(M-2)y^6-1035936My^5-2947563(M-2)y^4+3822918My^3+18538902(M-2)y^2-3536826My-54064629(M-2)\right)-6552(21y^{10}-287y^8+2188y^6-10748y^4+27367y^2-64109)\right)(G-A\sin(\alpha))^2-6486480(4a^2B^2(M(y(y(y(y(4y+7)-38)-98)+74)+427)-14(y^4-14y^2+61))+\Gamma(y^6-27y^4+323y^2-1385)))-6486480c_2(4a^2B^2(M(y(y(y(y(4y+7)-38)-98)+74)+427)-14(y^4-14y^2+61))+\Gamma(y^6-27y^4+323y^2-1385))-546c_1^2(132a^4B^4(M^2(y(y(y(y(y(y(y(7y+25)-83)-515)-209)+3643)+7111)-6737)-32714)+2M(y(6737-y(y(5y(y(y(5y+9)-103)-243)+3643)+14535))+62325)+90(y^6-27y^4+323y^2-1385))+12a^2B^2(3960(M(y(y(y(y(4y+7)-38)-98)+74)+427)-14(y^4-14y^2+61))+\Gamma(6My^9+11(M-2)y^8-214My^7-484(M-2)y^6+3614My^5+11066(M-2)y^4-27010My^3-129844(M-2)y^2+50804My+555731(M-2)))+\Gamma(11880(y^6-27y^4+323y^2-1385)+\Gamma(y^{10}-65y^8+2410y^6-53954y^4+631621y^2-2702765)))), \quad (57)$$

$$\Theta_2(y)=-\frac{1}{160059342643200B^2}(y^2-1)\gamma(G-\mathrm{A}\sin(\alpha))^2\left(\left(-\left((A^2+2G^2)M\left(a^2B^2\left(1576575My^{15}+2297295(M-2)y^{14}-31679505My^{13}-49808385(M-2)y^{12}+251771355My^{11}+443901195(M-2)y^{10}-866969541My^9-1717393941(M-2)y^8+732117949My^7+1691135469(M-2)y^6+2148126829My^5+5197726557(M-2)y^4-2312301143My^3-7951990023(M-2)y^2-2312301143My-7951990023(M-2)\right)-3392928(30y^{12}-425y^{10}+2851y^8-11384y^6+25198y^4-19847y^2-19847)\right)\gamma a^2\right)+AM\left(a^2B^2\left(1576575My^{15}+2297295(M-2)y^{14}-31679505My^{13}-49808385(M-2)y^{12}+251771355My^{11}+443901195(M-2)y^{10}-866969541My^9-1717393941(M-2)y^8+732117949My^7+1691135469(M-2)y^6+2148126829My^5+5197726557(M-2)y^4-2312301143My^3-7951990023(M-2)y^2-2312301143My-7951990023(M-2)\right)-3392928(30y^{12}-425y^{10}+2851y^8-11384y^6+25198y^4-19847y^2-19847)\right)\gamma(A\cos(2\alpha)+4G\sin(\alpha))a^2+882161280\left(a^2B^2\left(35My^7+45(M-2)y^6-325My^5-459(M-2)y^4+809My^3+1431(M-2)y^2+809My+1431(M-2)\right)-1512(y^4-4y^2+\right.$$

$11))\Big)c_4^2 + 205632\Big(4290\Big(a^2 B^2 \big(35My^7 + 45(M-2)y^6 - 325My^5 - 459(M-2)y^4 + 809My^3 + 1431(M-2)y^2 + 809My + 1431(M-2)\big) - 1512(y^4 - 4y^2 + 11)\Big) + \Big(39a^4 \big(70M^2 y^{10} + 210(M-2)My^9 - 14(M(61M+44)-44)y^8 - 3640(M-2)My^7 + (M(1621M+12254) - 12254)y^6 + 22100(M-2)My^5 + (M(15129M - 89386) + 89386)y^4 - 47728(M-2)My^3 + \big((257114 - 65391M)M - 257114\big)y^2 - 35518(M-2)My + M(257114 - 65391M) - 257114\big)B^4 + a^2 \Big(\big(165My^{11} + 195(M-2)y^{10} - 5451My^9 - 6669(M-2)y^8 + 79634My^7 + 102726(M-2)y^6 - 503806My^5 - 714090(M-2)y^4 + 1144841My^3 + 2033655(M-2)y^2 + 1144841My + 2033655(M-2)\big)\Gamma - 1287\big(140My^7 + 225(M-2)y^6 - 1300My^5 - 2715(M-2)y^4 + 3236My^3 + 8835(M-2)y^2 - 3484My - 22665(M-2)\big)\Big)B^2 - 1716(7y^8 - 173y^6 + 1717y^4 - 5423y^2 + 13792)\Gamma\Big)c_1\Big)c_4 + 882161280\Big(a^2 B^2 \big(35My^7 + 45(M-2)y^6 - 325My^5 - 459(M-2)y^4 + 809My^3 + 1431(M-2)y^2 + 809My + 1431(M-2)\big) - 1512(y^4 - 4y^2 + 11)\Big)c_5),$ (58)

The second order OHAM solution of velocity profile and temperature distribution are as under.

$$v_{OHAM}(y) = v_0(y) + v_1(y) + v_2(y) \tag{59}$$

and

$$\Theta_{OHAM}(y) = \Theta_0(y) + \Theta_1(y) + \Theta_2(y). \tag{60}$$

Using collocation method, we have found the values of c_1, c_2, c_4, c_5 for velocity profile as

c_1	c_2	c_4	c_5
-0.9721794673016152	-3.9622629501480556×10^{-4}	-1.3773239590060564	-0.6750848800383696

After using the values of c_i and $\gamma = 0.1, B = 0.1, a = 0.2, A = 0.4, \alpha = 165, M = 0.5, G = 1, \Gamma = 0.3$ in Eq. (59) we get

$v_{OHAM}(y) = -1.36845 \times 10^{-17}(-1 + y^2)(8.71528 \times 10^{15} + y(6.12648 \times 10^9 + y(-1.72871 \times 10^{15} + y(-3.14025 \times 10^9 + y(-8.41587 \times 10^{12} + y(3.2572 \times 10^8 + y(3.07209 \times 10^{11} + y(1.33903 \times 10^6 + y(5.70556 \times 10^8 + y(-37273.9 + y(-1.22634 \times 10^7 + y(-20.1364 + y(1.33903 \times 10^6 + y(5.70556 \times 10^8 + y(-37273.9 + y(-1.22634 \times 10^7 + y(-20.1364 + y(-62.6786 + 1y))))))))))))).$ (61)

Using the same method we have found the values of c_1, c_2, c_4, c_5 for temperature distribution as

c_1	c_2	c_4	c_5
0.8022157425325956	-2.6532547581107915	0.45512453948245185	-2.1169027772515703

Using the values of c_i and $\gamma = 0.1, B = 1, A = 0.5, \alpha = 165, M = 0.5, G = 1, \Gamma = 0.1$ in Eq. (60) we get

$\Theta_{OHAM}(y) = 0.664312 + y(0.5 + y(-0.223863 + y(-1.50995 \times 10^{-7} + y(0.0742752 + y(3.25779 \times 10^{-7} + y(-0.0146459 + y(-1.03106 \times 10^{-7} + y(-0.0000814195 + y(9.87488 \times 10^{-9} + y(3.14246 \times 10^{-6} + y(2.95234 \times 10^{-11} + y(3.16566 \times 10^{-10} + y(-8.63231 \times 10^{-13} + y(-1.82434 \times 10^{-11} + y(-1.19257 \times 10^{-16} + (-3.21288 \times 10^{-16} + 5.65363 \times 10^{-18}y)y))))))))))))))).$ (62)

4.2. HPM solution

Zero component of velocity and temperature distribution along with the boundary conditions are given by

$$\frac{d^4}{dy^4} v_0(y) + A\sin(\alpha) - G = 0, \tag{63}$$

$$v_0(y = \pm 1) = 0, \frac{d^2}{dy^2} v_0(y = \pm 1) = 0,$$

$$\frac{d^2}{dy^2} \Theta_0(y) = 0, \tag{64}$$

$$\Theta_0(y = -1) = 0, \Theta_0(y = 1) = 1.$$

Their solutions are

$$v_0(y) = \frac{1}{24}(5G - 6Gy^2 + Gy^4 - 5A\sin(\alpha) + 6Ay^2\sin(\alpha) - Ay^4\sin(\alpha)), \tag{65}$$

$$\Theta_0(y) = \frac{1+y}{2}. \tag{66}$$

First component of velocity and temperature distribution along with the boundary conditions are given by

$$a^2B^2M\frac{dv_0(y)}{dy}\frac{d\Theta_0(y)}{dy} + a^2B^2M\Theta_0(y)\frac{d^2v_0(y)}{dy^2} - a^2B^2\frac{d^2v_0(y)}{dy^2} + \Gamma v_0(y) + \frac{d^4v_1(y)}{dy^4} = 0, \tag{67}$$

$$v_1(y = \pm 1) = 0, \frac{d^2}{dy^2}v_1(y = \pm 1) = 0,$$

$$\frac{\gamma\left(\frac{d^2v_0(y)}{dy^2}\right)^2}{B^2} + \frac{\partial^2\Theta_1(y)}{dy^2} - a^2\gamma M\Theta_0(y)\left(\frac{dv_0(y)}{dy}\right)^2 + a^2\gamma\left(\frac{dv_0(y)}{dy}\right)^2 = 0, \tag{68}$$

$$\Theta_1(y = -1) = 0, \Theta_1(y = 1) = 0.\mathrm{b}$$

Their solutions are

$v_1(y) = \frac{1}{40320}(3416a^2AB^2\sin(\alpha) - 1708a^2AB^2M\sin(\alpha) + 16a^2AB^2My^7\sin(\alpha) + 28a^2AB^2My^6\sin(\alpha) - 168a^2AB^2My^5\sin(\alpha) - 420a^2AB^2My^4\sin(\alpha) +$

$$448a^2AB^2My^3\sin(\alpha) + 2100a^2AB^2My^2\sin(\alpha) - 296a^2AB^2My\sin(\alpha) - 56a^2AB^2y^6\sin(\alpha) + 840a^2AB^2y^4\sin(\alpha) - 4200a^2AB^2y^2\sin(\alpha) - 16a^2B^2GMy^7 - 28a^2B^2GMy^6 + 168a^2B^2GMy^5 + 420a^2B^2GMy^4 - 448a^2B^2GMy^3 - 2100a^2B^2GMy^2 + 296a^2B^2GMy + 1708a^2B^2GM + 56a^2B^2Gy^6 - 840a^2B^2Gy^4 + 4200a^2B^2Gy^2 - 3416a^2B^2G + 1385A\Gamma\sin(\alpha) + A\Gamma y^8\sin(\alpha) - 28A\Gamma y^6\sin(\alpha) + 350A\Gamma y^4\sin(\alpha) - 1708A\Gamma y^2\sin(\alpha) - 1385\Gamma G + \Gamma(-G)y^8 + 28\Gamma Gy^6 - 350\Gamma Gy^4 + 1708\Gamma Gy^2), \quad (69)$$

$$\Theta_1(y) = \frac{1}{181440B^2}(2862a^2A^2B^2\gamma\sin^2(\alpha) - 1431a^2A^2B^2\gamma M\sin^2(\alpha) + 35a^2A^2B^2\gamma My^9\sin^2(\alpha) + 45a^2A^2B^2\gamma My^8\sin^2(\alpha) - 360a^2A^2B^2\gamma My^7\sin^2(\alpha) - 504a^2A^2B^2\gamma My^6\sin^2(\alpha) + 1134a^2A^2B^2\gamma My^5\sin^2(\alpha) + 1890a^2A^2B^2\gamma My^4\sin^2(\alpha) - 809a^2A^2B^2\gamma My\sin^2(\alpha) - 90a^2A^2B^2\gamma y^8\sin^2(\alpha) + 1008a^2A^2B^2\gamma y^6\sin^2(\alpha) - 3780a^2A^2B^2\gamma y^4\sin^2(\alpha) - 5724a^2AB^2\gamma G\sin(\alpha) + 2862a^2AB^2\gamma GM\sin(\alpha) - 70a^2AB^2\gamma GMy^9\sin(\alpha) - 90a^2AB^2\gamma GMy^8\sin(\alpha) + 720a^2AB^2\gamma GMy^7\sin(\alpha) + 1008a^2AB^2\gamma GMy^6\sin(\alpha) - 2268a^2AB^2\gamma GMy^5\sin(\alpha) - 3780a^2AB^2\gamma GMy^4\sin(\alpha) + 1618a^2AB^2\gamma GMy\sin(\alpha) + 180a^2AB^2\gamma Gy^8\sin(\alpha) - 2016a^2AB^2\gamma Gy^6\sin(\alpha) + 7560a^2AB^2\gamma Gy^4\sin(\alpha) + 2862a^2B^2\gamma G^2 - 1431a^2B^2\gamma G^2M + 35a^2B^2\gamma G^2My^9 + 45a^2B^2\gamma G^2My^8 - 360a^2B^2\gamma G^2My^7 - 504a^2B^2\gamma G^2My^6 + 1134a^2B^2\gamma G^2My^5 + 1890a^2B^2\gamma G^2My^4 - 809a^2B^2\gamma G^2My - 90a^2B^2\gamma G^2y^8 + 1008a^2B^2\gamma G^2y^6 - 3780a^2B^2\gamma G^2y^4 + 16632A^2\gamma\sin^2(\alpha) - 1512A^2\gamma y^6\sin^2(\alpha) + 7560A^2\gamma y^4\sin^2(\alpha) - 22680A^2\gamma y^2\sin^2(\alpha) - 33264A\gamma G\sin(\alpha) + 3024A\gamma Gy^6\sin(\alpha) - 15120A\gamma Gy^4\sin(\alpha) + 45360A\gamma Gy^2\sin(\alpha) + 16632\gamma G^2 - 1512\gamma G^2y^6 + 7560\gamma G^2y^4 - 22680\gamma G^2y^2), \quad (70)$$

Second component of velocity and temperature distribution along with the boundary conditions are given by

$$a^2B^2M\Theta_0(y)\frac{d^2v_1(y)}{dy^2}a^2B^2M\Theta_1(y)\frac{d^2v_0(y)}{dy^2} - a^2B^2\frac{d^2v_1(y)}{dy^2} + \frac{d^4v_2(y)}{dy^4}a^2B^2M\frac{dv_1(y)}{dy}\frac{d\Theta_0(y)}{dy} + a^2B^2M\frac{dv_0(y)}{dy}\frac{d\Theta_1(y)}{dy} + \Gamma v_1(y) = 0, \quad (71)$$

$$v_2(y=\pm1) = 0, \frac{d^2}{dy^2}v_2(y=\pm1) = 0,$$

$$\frac{2\gamma\frac{d^2v_0(y)}{dy^2}\frac{d^2v_1(y)}{dy^2}}{B^2} + \frac{d^2\Theta_2(y)}{dy^2} + 2a^2\gamma M\Theta_0(y)\frac{dv_0(y)}{dy}\frac{dv_1(y)}{dy} - a^2\gamma M\Theta_1(y)\left(\frac{dv_0(y)}{dy}\right)^2 + 2a^2\gamma\frac{dv_0(y)}{dy}\frac{dv_1(y)}{dy} = 0, \quad (72)$$

$$\Theta_2(y=-1) = 0, \Theta_2(y=1) = 0.$$

Their solutions are

$$v_2(y) = \frac{1}{261534873600}((y^2-1)(G - A\sin(\alpha))(a^4B^2(72072B^2(M^2(y(y(y(y(y(y(y(7y + 25) - 83) - 515) - 209) + 3643) + 7111) - 6737) - 32714) + 2M(y(6737 - y(y(5y(y(y(5y+9) - 103) - 243) + 3643) + 14535)) + 62325) + 90(y^6 - 27y^4 + 323y^2 - 1385)) - \gamma M(A^2+2G^2)(1540My^{13} + 2475(M-2)y^{12} - 31010My^{11} - 55674(M-2)y^{10} + 237622My^9 + 511893(M-2)y^8 - 573188My^7 - 1515132(M-2)y^6 - 1035936My^5 - 2947563(M-2)y^4 + 3822918My^3 + 18538902(M-2)y^2 - 3536826My - 54064629(M-2))) + 6552a^2(\gamma M(21y^{10} - 287y^8 + 2188y^6 - 10748y^4 + 27367y^2 - 64109)(A^2+2G^2) + B^2\Gamma(6My^9 + 11(M-2)y^8 - 214My^7 - 484(M-2)y^6 + 3614My^5 + 11066(M-2)y^4 - 27010My^3 - 129844(M-2)y^2 + 50804My + 555731(M-2))) + a^2A\gamma M(a^2B^2(1540My^{13} + 2475(M-2)y^{12} - 31010My^{11} - 55674(M-2)y^{10} + 237622My^9 + 511893(M-2)y^8 - 573188My^7 - 1515132(M-2)y^6 - 1035936My^5 - 2947563(M-2)y^4 + 3822918My^3 + 18538902(M-2)y^2 - 3536826My - 54064629(M-2)) - 6552(21y^{10} - 287y^8 + 2188y^6 - 10748y^4 + 27367y^2 - 64109))(A\cos(2\alpha) + 4G\sin(\alpha)) + 546\Gamma^2(y^{10} - 65y^8 + 2410y^6 - 53954y^4 + 631621y^2 - 2702765))), \quad (73)$$

$$\Theta_2(y) = \frac{1}{160059342643200B^2}(\gamma(y^2 - 1)(G - A\sin(\alpha))^2(a^4B^2(\gamma M(A^2+2G^2)(1576575My^{15} + 2297295(M-2)y^{14} - 31679505My^{13} - 49808385(M-2)y^{12} + 251771355My^{11} + 443901195(M-2)y^{10} - 866969541My^9 - 1717393941(M-2)y^8 + 732117949My^7 + 1691135469(M-2)y^6 + 2148126829My^5 + 5197726557(M-2)y^4 - 2312301143My^3 - 7951990023(M-2)y^2 - 2312301143My - 7951990023(M-2)) - 8019648B^2(70M^2y^{10} + 210(M-2)My^9 - 14(M(61M+44) - 44)y^8 - 3640(M-2)My^7 + (M(1621M+12254) - 12254)y^6 + 22100(M-2)My^5 + (M(15129M - 89386) + 89386)y^4 - 47728(M-2)My^3 + ((257114 - 65391M)M - 257114)y^2 - 35518(M-2)My + M(257114 - 65391M) - 257114)) - 102816a^2(33\gamma M(30y^{12} - 425y^{10} + 2851y^8 - 11384y^6 + 25198y^4 - 19847y^2 - 19847)(A^2+2G^2) + 2B^2(\Gamma(165My^{11} + 195(M-2)y^{10} - 5451My^9 - 6669(M-2)y^8 + 79634My^7 + 102726(M-2)y^6 - 503806My^5 - 714090(M-2)y^4 + 1144841My^3 + 2033655(M-2)y^2 + 1144841My + 2033655(M-2)) - 1287(140My^7 + 225(M-2)y^6 - 1300My^5 - 2715(M-2)y^4 + 3236My^3 + 8835(M-2)y^2 -$$

$$3484My - 22665(M-2)\Big)\Big)\Big) - a^2A\gamma M\Big(a^2B^2\big(1576575My^{15} + 2297295(M-2)y^{14} - 31679505My^{13} - 49808385(M-2)y^{12} + 251771355My^{11} + 443901195(M-2)y^{10} - 866969541My^9 - 1717393941(M-2)y^8 + 732117949My^7 + 1691135469(M-2)y^6 + 2148126829My^5 + 5197726557(M-2)y^4 - 2312301143My^3 - 7951990023(M-2)y^2 - 2312301143My - 7951990023(M-2)\big) - 3392928(30y^{12} - 425y^{10} + 2851y^8 - 11384y^6 + 25198y^4 - 19847y^2 - 19847)\Big)(A\cos(2\alpha) + 4G\sin(\alpha)) + 352864512\Gamma(7y^8 - 173y^6 + 1717y^4 - 5423y^2 + 13792)\Big)\Big). \quad (74)$$

The second order HPM solution of velocity profile and temperature distribution are as under.

$$v_{HPM}(y) = v_0(y) + v_1(y) + v_2(y). \quad (75)$$

and

$$\Theta_{HPM}(y) = \Theta_0(y) + \Theta_1(y) + \Theta_2(y). \quad (76)$$

Using of $\gamma = 0.1, \mathrm{B} = 0.1, \mathrm{A} = 0.04, \alpha = 135, \mathrm{M} = 0.005, \mathrm{G} = 1, \Gamma = 0.01, \mathrm{a} = 0.2$ in Eq. (75) and Eq. (76) one obtains the following solutions.

$$v_{HPM}(y)=0.207222 + y(1.46023 \times 10^{-8} + y(-0.248654 + y(-2.21003 \times 10^{-8} + y(0.0414248 + y(8.28676 \times 10^{-9} + y(7.44514 \times 10^{-6} + y(-7.88697 \times 10^{-10} + y(-2.44068 \times 10^{-7} + y(-1.20551 \times 10^{-13} + y(-3.21233 \times 10^{-10} + y(2.91432 \times 10^{-15} + y(2.10224 \times 10^{-11} + y(9.8514 \times 10^{-18} + (2.98879 \times 10^{-16} - 4.66088 \times 10^{-19}y)y)))))))))))))), \quad (77)$$

and

$$\Theta_{HPM}(y) =1.40694 + y(0.5 + y(-1.23656 + y(-2.20644 \times 10^{-7} + y(0.41193 + y(2.72583 \times 10^{-7} + y(-0.0822714 + y(-8.65162 \times 10^{-8} + y(-0.0000441843 + y(8.403 \times 10^{-9} + y(1.50419 \times 10^{-6} + y(1.59405 \times 10^{-12} + y(3.82264 \times 10^{-9} + y(-4.06999 \times 10^{-14} + y(-2.50695 \times 10^{-10} + y(-1.63881 \times 10^{-16} + (-4.51697 \times 10^{-15} + 7.76913 \times 10^{-18}y)y)))))))))))))))). \quad (78)$$

4.3. Volumetric flux, average velocity, shear stress, skin friction

Dimensionless representation of the volume flux can be expressed as

$$Q = \int_{-1}^{1} v(y)dy. \quad (79)$$

By plugging in Eq.(61) and (77) into Eq.(79), we get the following equations

$$Q_{OHAM} = -\frac{1}{261534873600}\big((G - A\sin(\alpha))(a^4B^2(B^2((1.08116 \times 10^{10} - 2.844 \times 10^9 M)M - 1.08116 \times 10^{10}) + \gamma G^2 M(1.80917 \times 10^8 M - 3.61833 \times 10^8)) + a^2A\gamma M\sin(\alpha)(A\sin(\alpha)(a^2B^2(1.80917 \times 10^8 M - 3.61833 \times 10^8) - 1.3911 \times 10^9) + G(a^2B^2(7.23667 \times 10^8 - 3.61833 \times 10^8 M) + 2.78219 \times 10^9)) + a^2(B^2(-8.76344 \times 10^9\Gamma + (4.38172 \times 10^9\Gamma - 1.41092 \times 10^{10})M + 2.82185 \times 10^{10}) - 1.3911 \times 10^9\gamma G^2 M) + \Gamma(1.14349 \times 10^{10} - 1.77584 \times 10^9\Gamma) - 6.97426 \times 10^{10})\big), \quad (80)$$

$$Q_{HPM} = -\frac{1}{85135050}\big((G - A\sin(\alpha))(a^4B^2(21991\gamma(M-2)M(A^2 + 2G^2) - 1092B^2(M(897M - 3410) + 3410)) + 42a^2(13B^2(2764\Gamma - 8415)(M-2) - 4026\gamma M(A^2 + 2G^2)) - a^2A\gamma M(21991a^2B^2(M-2) - 169092)(A\cos(2\alpha) + 4G\sin(\alpha)) - 56(\Gamma(10922\Gamma - 66495) + 405405))\big). \quad (81)$$

The couple stress fluid's average velocity is represented by the symbol $\bar{v}$ and its definition is as follows:

$$\bar{v} = \frac{Q}{d}. \quad (82)$$

Dimensionless form of (82) correspondence with the flow rate given in (80) and (81).

On the surface of the upper plate, the dimensionless shear stress S_p may be calculated using the following formula:

$$S_p = -\mu\frac{dv}{dy}\Big|_{y=1}. \quad (83)$$

In this case, there is a minus sign because the top plate is pointing in the negative y direction of the coordinate system. Putting v_{OHAM} and v_{HPM} in (83) we get the following equations:

$$S_{OHAM} = \frac{1}{130767436800}\big(\mu(G - A\sin(\alpha))(c_1(2a^2\gamma c_4 M(a^2B^2(-39529728(M-2) - 1114880M) + 298561536)(G - A\sin(\alpha))^2 - 12972960(4a^2B^2(376M - 672) - 1088\Gamma)) - 6486480(c_2(4a^2B^2(336(M-2) + 40M) - 1088\Gamma) - 6720) - 546c_1^2(132a^4B^4(-29472M^2 + 105088M - 97920) + 12a^2B^2(\Gamma(436480(M-2) + 27200M) + 3960(376M - 672)) + \Gamma(-2122752\Gamma - 12925440)))\big), \quad (84)$$

$$S_{HPM} = -\frac{1}{510810300}\big(\mu(G - A\sin(\alpha))(a^4B^2(2\gamma M(79384M - 154413)(A^2 + 2G^2) - 9009B^2(M(921M - 3284) + 3060)) - 1638a^2(712\gamma M(A^2 + 2G^2) + 5B^2(44(62\Gamma - 189) + 9(517 - 161\Gamma)M)) - 2a^2A\gamma M(a^2B^2(79384M - 154413) - 583128)(A\cos(2\alpha) + 4G\sin(\alpha)) - 3276(\Gamma(1382\Gamma - 8415) + 51975))\big). \quad (85)$$

The opposite resistive force which is created between the surface of the body and particles of the fluid is called skin friction coefficient. The formula given below represents the skin friction coefficient at both plates.

$$\Theta'(y) = \frac{1.328}{\sqrt{\frac{\rho v H}{\mu}}}.$$

The volume fluxes that were calculated using OHAM and HPM are denoted here by Q_{OHAM} and Q_{HPM} respectively. Moreover, Eqs. (84) and (85) represents the shear stresses obtained by putting v_{OHAM} & v_{HPM} in eq. (83).

DOI 10.2478/ama-2024-0058

5. RESULTS AND DISCUSSION

Throughout the course of this investigation, we monitored the flow of couple stress fluids as heat was transferred between two inclined plates that were parallel to one another. Analytical models of the velocity field and temperature distribution were built with the help of the OHAM and HPM. In this scenario, the impacts of several non-dimensional parameters on the velocity field, temperature distribution, volumetric flow rate, and shear stress are visually depicted. Tables 1 - 5 display OHAM and HPM solutions for fluid velocity, temperature distributions, residuals, absolute differences and skin friction for both approaches. It has been demonstrated that OHAM and HPM yield comparable outcomes.

Tab. 1. Comparing the results of OHAM & HPM for velocity profile, when $\gamma = 0.2, A = 0.4, B = 0.1, a = 0.2, \alpha = 165, M = 0.01, G\ 1, \Gamma = 0.3$.

y	v_{OHAM}	Residual v_{OHAM}	v_{HPM}	Residual v_{HPM}	Average Residual
-1.	0.	-2.72735×10^{-9}	1.82554×10^{-17}	-1.0742×10^{-7}	5.50735×10^{-8}
-0.9	0.0190055	-5.93355×10^{-9}	0.0190078	1.43614×10^{-5}	7.17775×10^{-6}
-0.8	0.037468	-1.78626×10^{-8}	0.0374725	2.84835×10^{-5}	1.42328×10^{-5}
-0.7	0.054899	-4.10482×10^{-8}	0.0549056	4.19107×10^{-5}	2.09348×10^{-5}
-0.6	0.070869	-7.42714×10^{-8}	0.0708775	5.43114×10^{-5}	2.71186×10^{-5}
-0.5	0.085007	-1.1398×10^{-7}	0.0850172	6.53782×10^{-5}	3.26321×10^{-5}
-0.4	0.0969998	-1.55482×10^{-7}	0.0970115	7.48361×10^{-5}	3.73403×10^{-5}
-0.3	0.106592	-1.93888×10^{-7}	0.106605	8.24494×10^{-5}	4.11278×10^{-5}
-0.2	0.113585	-2.24802×10^{-7}	0.113599	8.80278×10^{-5}	4.39015×10^{-5}
-0.1	0.117837	-2.44795×10^{-7}	0.117851	9.14316×10^{-5}	4.55934×10^{-5}
0.	0.119264	-2.51702×10^{-7}	0.119278	9.25755×10^{-5}	4.61619×10^{-5}
0.1	0.117837	-2.44786×10^{-7}	0.117851	9.14309×10^{-5}	4.55931×10^{-5}
0.2	0.113585	-2.24786×10^{-7}	0.113599	8.80265×10^{-5}	4.39008×10^{-5}
0.3	0.106592	-1.93866×10^{-7}	0.106605	8.24476×10^{-5}	4.11268×10^{-5}
0.4	0.0969998	-1.55457×10^{-7}	0.0970115	7.48339×10^{-5}	3.73392×10^{-5}
0.5	0.085007	-1.13957×10^{-7}	0.0850172	6.53756×10^{-5}	3.26308×10^{-5}
0.6	0.070869	-7.4254×10^{-8}	0.0708776	5.43086×10^{-5}	2.71172×10^{-5}
0.7	0.054899	-4.10381×10^{-8}	0.0549056	4.19079×10^{-5}	2.09334×10^{-5}
0.8	0.037468	-1.78602×10^{-8}	0.0374725	2.84808×10^{-5}	1.42315×10^{-5}
0.9	0.0190055	-5.93575×10^{-9}	0.0190078	1.4359×10^{-5}	7.17655×10^{-6}
1.	0.	-2.72655×10^{-9}	1.75113×10^{-17}	-1.09349×10^{-7}	5.6038×10^{-8}

Tab. 2. Comparing the results of OHAM & HPM for temperature distribution, when $\gamma = 0.03, A = 0.004, B = 0.1, \alpha = 135, M = 0.00005, G = 0.1, \Gamma = 0.01, a = 0.2$.

y	Θ_{OHAM}	Residual Θ_{OHAM}	Θ_{HPM}	Residual Θ_{HPM}	Average Residual
-1.	-1.06962×10^{-19}	4.58588×10^{-10}	-9.06168×10^{-19}	1.2674×10^{-11}	2.35631×10^{-10}
-0.9	0.0503963	9.85987×10^{-8}	0.0503956	2.13349×10^{-9}	5.03661×10^{-8}
-0.8	0.10079	3.47926×10^{-7}	0.100788	8.04974×10^{-9}	1.77988×10^{-7}
-0.7	0.151173	6.89008×10^{-7}	0.151171	1.69256×10^{-8}	3.52967×10^{-7}
-0.6	0.201537	1.07253×10^{-6}	0.201534	2.77568×10^{-8}	5.50143×10^{-7}
-0.5	0.25187	1.45826×10^{-6}	0.251867	3.94455×10^{-8}	7.48854×10^{-7}
-0.4	0.302162	1.81409×10^{-6}	0.302158	5.08813×10^{-8}	9.32485×10^{-7}
-0.3	0.352401	2.11508×10^{-6}	0.352397	6.1022×10^{-8}	1.08805×10^{-6}

-0.2	0.402579	2.34273×10^{-6}	0.402574	6.89681×10^{-8}	1.20585×10^{-6}
-0.1	0.452689	2.48428×10^{-6}	0.452684	7.40271×10^{-8}	1.27915×10^{-6}
0.	0.502726	2.53228×10^{-6}	0.502721	7.5763×10^{-8}	1.30402×10^{-6}
0.1	0.552689	2.48428×10^{-6}	0.552684	7.40271×10^{-8}	1.27915×10^{-6}
0.2	0.602579	2.34273×10^{-6}	0.602574	6.8968×10^{-8}	1.20585×10^{-6}
0.3	0.652401	2.11508×10^{-6}	0.652397	6.1022×10^{-8}	1.08805×10^{-6}
0.4	0.702162	1.81409×10^{-6}	0.702158	5.08813×10^{-8}	9.32486×10^{-7}
0.5	0.75187	1.45826×10^{-6}	0.751867	3.94454×10^{-8}	7.48855×10^{-7}
0.6	0.801537	1.07253×10^{-6}	0.801534	2.77567×10^{-8}	5.50143×10^{-7}
0.7	0.851173	6.89009×10^{-7}	0.851171	1.69256×10^{-8}	3.52967×10^{-7}
0.8	0.90079	3.47927×10^{-7}	0.900788	8.04971×10^{-9}	1.77988×10^{-7}
0.9	0.950396	9.85988×10^{-8}	0.950396	2.13348×10^{-9}	5.03661×10^{-8}
1.	1.	4.58565×10^{-10}	1.	1.26734×10^{-11}	2.35619×10^{-10}

Tab. 3. Comparison of OHAM & HPM for velocity profile, when $\gamma = 0.2, A = 0.04, B = 0.1, a = 0.2, \alpha = 165, M = 0.05, G = 1, \Gamma = 0.3$.

y	v_{OHAM}	v_{HPM}	**Absolute Difference**
-1.	0.	-7.32191×10^{-19}	1.01466×10^{-17}
-0.9	0.0303673	0.0303708	3.57024×10^{-6}
-0.8	0.0598669	0.059874	7.05155×10^{-6}
-0.7	0.0877185	0.0877288	1.03576×10^{-5}
-0.6	0.113236	0.113249	1.3407×10^{-5}
-0.5	0.135826	0.135842	1.61247×10^{-5}
-0.4	0.154988	0.155006	1.84444×10^{-5}
-0.3	0.170314	0.170335	2.03097×10^{-5}
-0.2	0.181488	0.181509	2.16752×10^{-5}
-0.1	0.188282	0.188305	2.2508×10^{-5}
0.	0.190562	0.190585	2.27878×10^{-5}
0.1	0.188282	0.188305	2.25079×10^{-5}
0.2	0.181488	0.181509	2.16751×10^{-5}
0.3	0.170314	0.170335	2.03095×10^{-5}
0.4	0.154988	0.155006	1.84442×10^{-5}
0.5	0.135826	0.135842	1.61245×10^{-5}
0.6	0.113236	0.113249	1.34067×10^{-5}
0.7	0.0877185	0.0877289	1.03574×10^{-5}
0.8	0.059867	0.059874	7.05141×10^{-6}
0.9	0.0303673	0.0303709	3.57017×10^{-6}
1.	0.	-8.61145×10^{-20}	1.09648×10^{-17}

Tab. 4. Comparison of OHAM & HPM for temperature distribution, when $\gamma = 0.03, A = 0.04, B = 0.1, \alpha = 135, M = 0.00005, G = 0.1, \Gamma = 0.01, a = 0.2$.

y	Θ_{OHAM}	Θ_{HPM}	**Absolute Difference**
-1.	-1.06962×10^{-19}	-9.06168×10^{-19}	5.96311×10^{-19}
-0.9	0.0503963	0.0503956	7.16137×10^{-7}
-0.8	0.10079	0.100788	1.42771×10^{-6}

DOI 10.2478/ama-2024-0058

-0.7	0.151173	0.151171	2.12385×10^{-6}
-0.6	0.201537	0.201534	2.78821×10^{-6}
-0.5	0.25187	0.251867	3.40088×10^{-6}
-0.4	0.302162	0.302158	3.9404×10^{-6}
-0.3	0.352401	0.352397	4.38587×10^{-6}
-0.2	0.402579	0.402574	4.71879×10^{-6}
-0.1	0.452689	0.452684	4.92468×10^{-6}
0.	0.502726	0.502721	4.99437×10^{-6}
0.1	0.552689	0.552684	4.92468×10^{-6}
0.2	0.602579	0.602574	4.71879×10^{-6}
0.3	0.652401	0.652397	4.38587×10^{-6}
0.4	0.702162	0.702158	3.9404×10^{-6}
0.5	0.75187	0.751867	3.40087×10^{-6}
0.6	0.801537	0.801534	2.78821×10^{-6}
0.7	0.851173	0.851171	2.12385×10^{-6}
0.8	0.90079	0.900788	1.42771×10^{-6}
0.9	0.950396	0.950396	7.16137×10^{-7}
1.	1.	1.	1.62664×10^{-17}

Tab. 5. Calculations for $\Theta'(-1)$ and $\Theta'(1)$ against different values of γ keeping $G = 0.001, a = 0.2, M = 0.00015, \alpha = 155, A = 0.02, \Gamma = 0.02, B = 0.3$ fixed.

γ	$\Theta'_{OHAM}(-1)$	$\Theta'_{HPM}(-1)$	Absolute Difference	$\Theta'_{OHAM}(1)$	$\Theta'_{HPM}(1)$	Absolute Difference
-1.	0.499496	0.499499	2.79823×10^{-6}	0.500504	0.500501	2.79821×10^{-6}
-0.877	0.499558	0.499561	2.45405×10^{-6}	0.500442	0.500439	2.45403×10^{-6}
-0.754	0.49962	0.499622	2.10986×10^{-6}	0.50038	0.500378	2.10985×10^{-6}
-0.631	0.499682	0.499684	1.76568×10^{-6}	0.500318	0.500316	1.76567×10^{-6}
-0.508	0.499744	0.499745	1.4215×10^{-6}	0.500256	0.500255	1.42149×10^{-6}
-0.385	0.499806	0.499807	1.07732×10^{-6}	0.500194	0.500193	1.07731×10^{-6}
-0.262	0.499868	0.499869	7.33135×10^{-7}	0.500132	0.500131	7.33132×10^{-7}
-0.139	0.49993	0.49993	3.88954×10^{-7}	0.50007	0.50007	3.88952×10^{-7}
-0.016	0.499992	0.499992	4.47716×10^{-8}	0.500008	0.500008	4.47714×10^{-8}
0.107	0.500054	0.500054	2.9941×10^{-7}	0.499946	0.499946	2.99409×10^{-7}
0.23	0.500116	0.500115	6.43592×10^{-7}	0.499884	0.499885	6.43589×10^{-7}
0.353	0.500178	0.500177	9.87774×10^{-7}	0.499822	0.499823	9.8777×10^{-7}
0.476	0.50024	0.500239	1.33196×10^{-6}	0.49976	0.499761	1.33195×10^{-6}
0.599	0.500302	0.5003	1.67614×10^{-6}	0.499698	0.4997	1.67613×10^{-6}
0.722	0.500364	0.500362	2.02032×10^{-6}	0.499636	0.499638	2.02031×10^{-6}
0.845	0.500426	0.500423	2.3645×10^{-6}	0.499574	0.499577	2.36449×10^{-6}
0.968	0.500488	0.500485	2.70868×10^{-6}	0.499512	0.499515	2.70867×10^{-6}

sciendo
DOI 10.2478/ama-2024-0058 acta mechanica et automatica, vol.18 no.3 (2024)

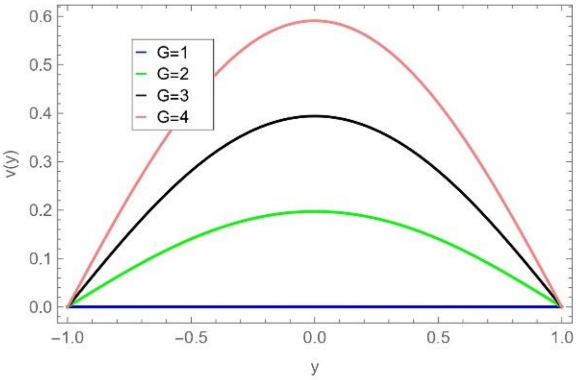

Fig. 2. Velocity Profile for $B = 2.5, \gamma = 2, A = 1, a = 0.1, \alpha = 165, M = 0.002, \Gamma = 0.2$ using OHAM

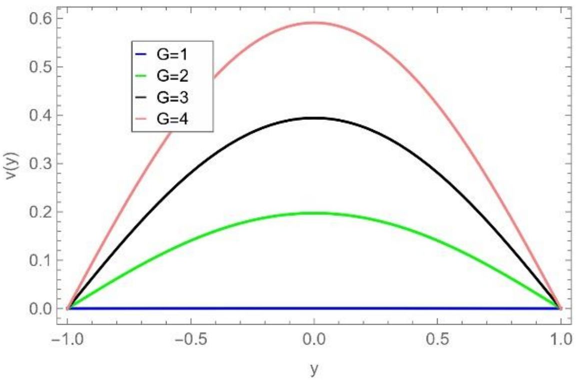

Fig. 3. Velocity Profile for $B = 2.5, \gamma = 2, A = 1, a = 0.1, \alpha = 165, M = 0.002, \Gamma = 0.2$ using HPM

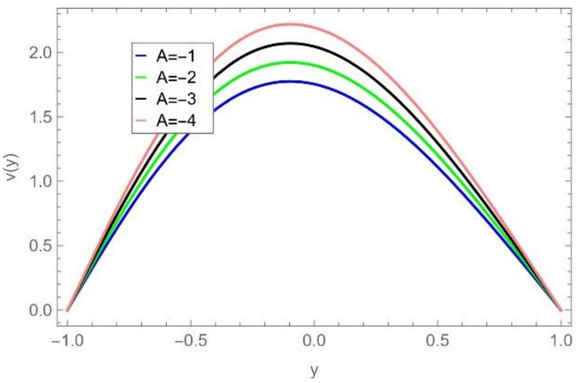

Fig. 4. Velocity Profile for $B = 1.4, \gamma = 0.1, G = 1, \alpha = 135, a = 3, M = 1.15, \Gamma = 0.2$ using OHAM

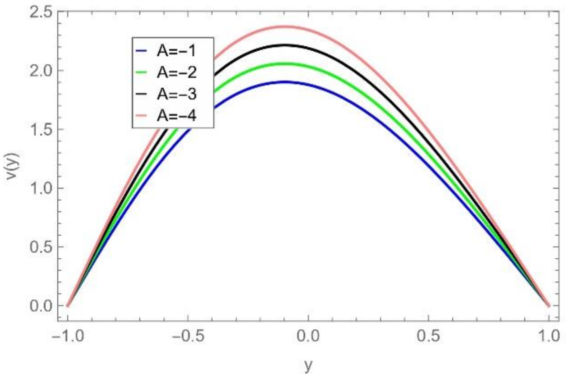

Fig. 5. Velocity Profile for $B = 1.4, \gamma = 0.1, G = 1, \alpha = 135, a = 3, M = 1.15, \Gamma = 0.2$ using HPM

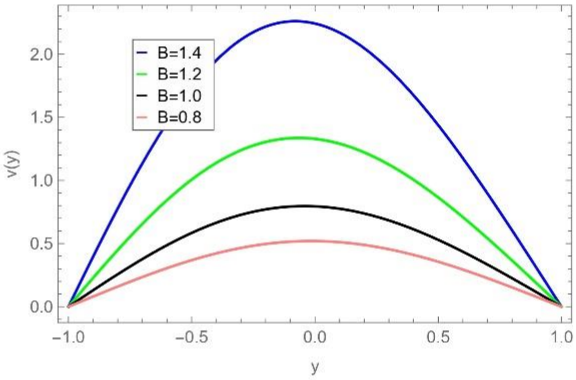

Fig. 6. Velocity Profile for $G = 1, \gamma = 3, A = -1, a = 3\ \alpha = 135, M = 1.15, \Gamma = 0.2$ using OHAM

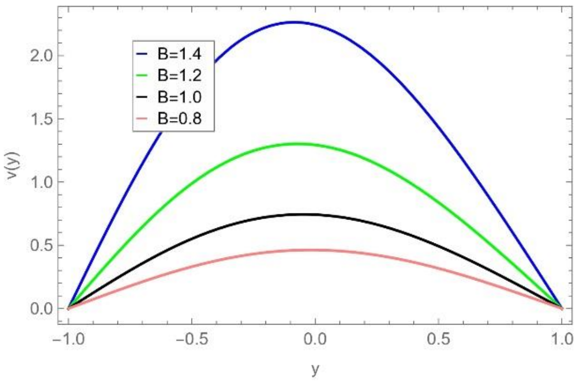

Fig. 7. Velocity Profile for $G = 1, \gamma = 3, A = -1, a = 3\ \alpha = 135, M = 1.15, \Gamma = 0.2$ using HPM

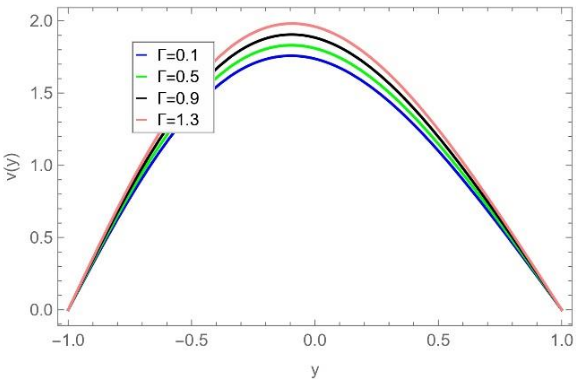

Fig. 8. Velocity Profile for $G = 1, \gamma = 0.1, A = -1, a = 3, \alpha = 135, M = 1.15, B = 1.4$ using OHAM

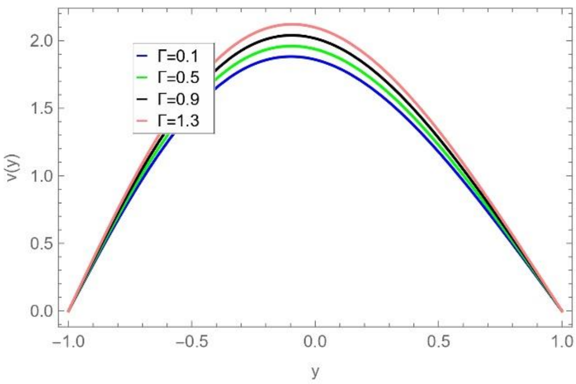

Fig. 9. Velocity Profile for $G = 1, \gamma = 0.1, A = -1, a = 3, \alpha = 135, M = 1.15, B = 1.4$ using HPM

DOI 10.2478/ama-2024-0058

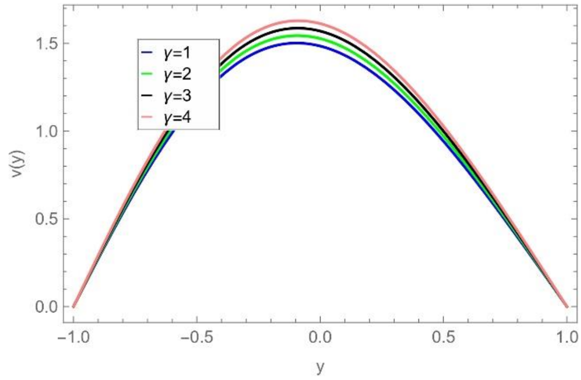

Fig. 10. Velocity Profile for $B = 2.1, A = 1.1, G = 1, \alpha = 13, a = 2, M = 1.15, \Gamma = 0.2$ using OHAM

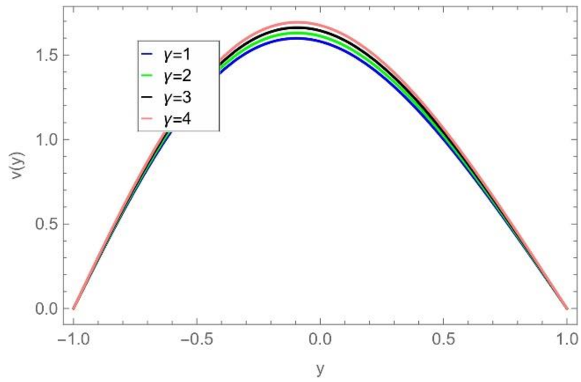

Fig. 11. Velocity Profile for $B = 2.1, A = 1.1, G = 1, \alpha = 13, a = 2, M = 1.15, \Gamma = 0.2$ using HPM

Figures 2-11 for the velocity profile in the case of inclined Poiseuille flow are presented to explore the impacts of various parameters. As we can see in these graphs, changes in parameter values create changes in fluid velocity. Both Figures 4 and 5 show that the pressure gradient A is inversely proportional to the fluid's velocity. The results of parameter B's influence on the flow velocity are shown in Figures 6 and 7. If you raise B, the fluid's velocity goes up, and if you lower B, it slows down. The impact of the MHD parameter Γ on the velocity field is seen in Figures 8 and 9. The fluid's velocity and Γ are directly related to one another. The MHD parameter controls the relationship between magnetic fields and fluid velocity on an inclined plane. Increased parameter values modify velocity profiles and flow stability by amplifying magnetic effects.

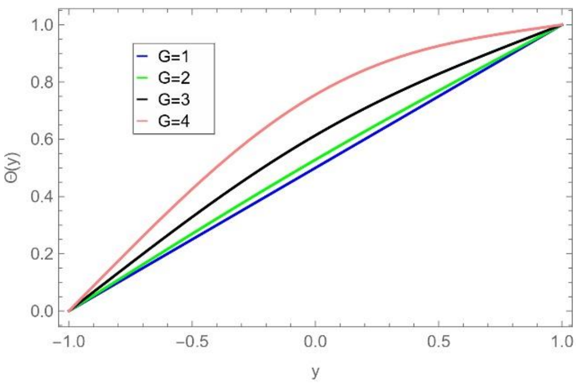

Fig. 12. Temperature distribution for $B = 2.5, \gamma = 2, A = 1, a = 0.1, \alpha = 165, M = 0.002, \Gamma = 0.2$ using OHAM

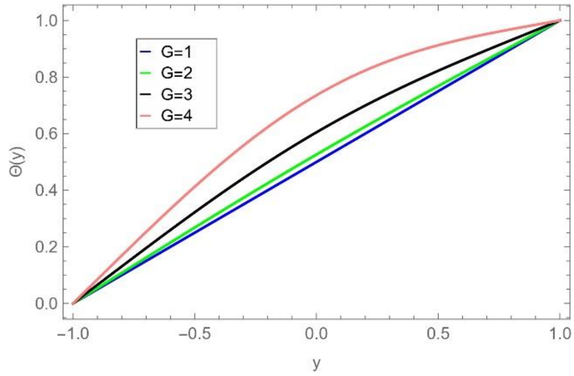

Fig. 13. Temperature distribution for $B = 2.5, \gamma = 2, A = 1, a = 0.1, \alpha = 165, M = 0.002, \Gamma = 0.2$ using HPM

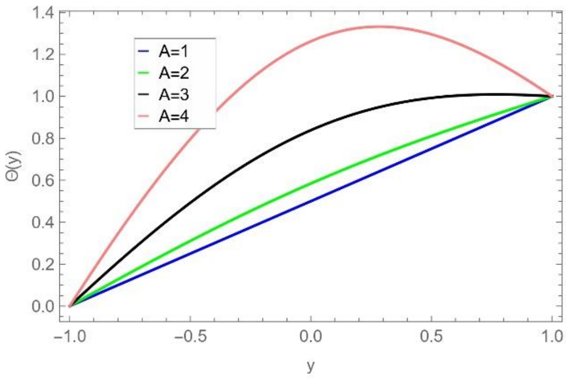

Fig. 14. Temperature distribution for $B = 0.3, \gamma = 0.1, G = 1, \alpha = 165, a = 3, M = 0.015, \Gamma = 0.2$ using OHAM

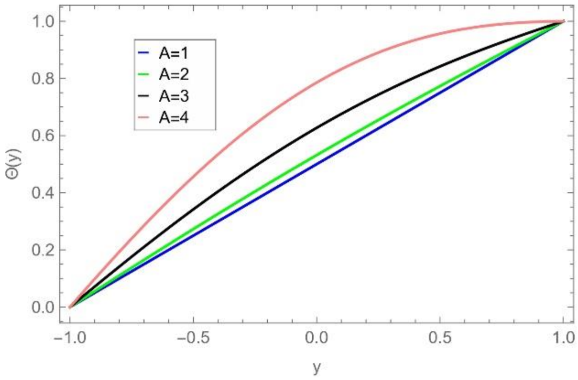

Fig. 15. Temperature distribution for $B = 0.3, \gamma = 0.1, G = 1, \alpha = 165, a = 3, M = 0.015, \Gamma = 0.2$ using HPM

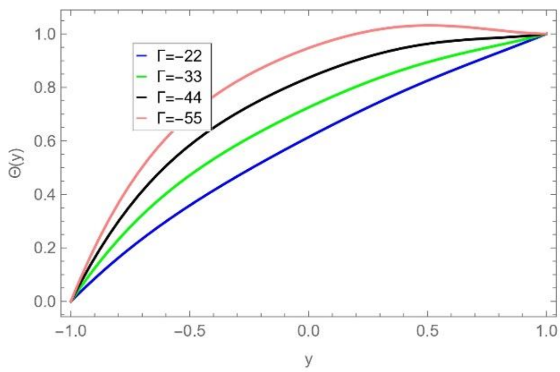

Fig. 16. Temperature distribution for $G = 2, \gamma = 0.2, A = 0.3, a = 3, \alpha = 135, M = 1.15, B = 1.4$ using OHAM

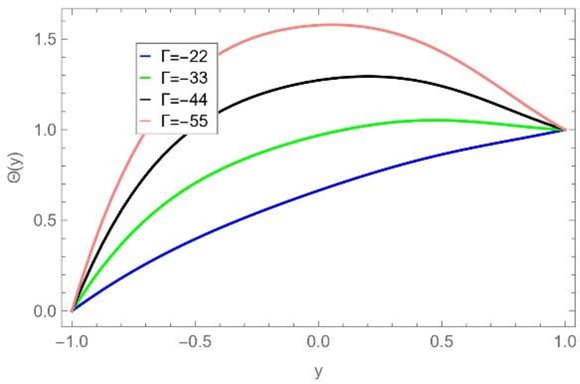

Fig. 17. Temperature distribution for $G = 2, \gamma = 0.2, A = 0.3, a = 3, \alpha = 135, M = 1.15, B = 1.4$ using HPM

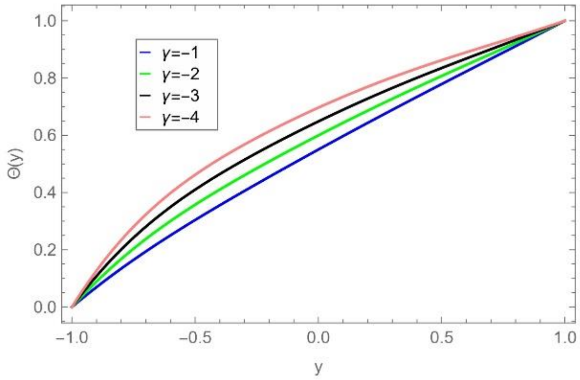

Fig. 18. Temperature distribution for $B = 2.1, A = 1.1, G = 1, \alpha = 135, a = 2, M = 1.15, \Gamma = 0.2$ using OHAM

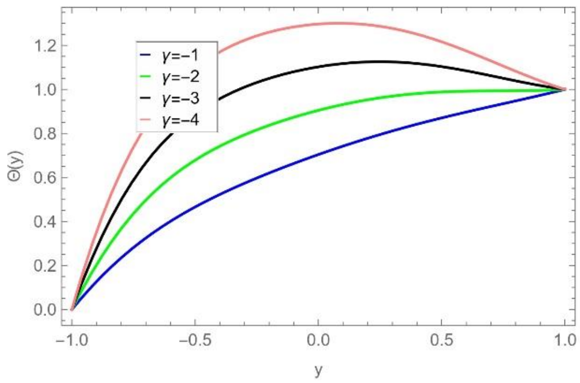

Fig. 19. Temperature distribution for $B = 2.1, A = 1.1, G = 1, \alpha = 135, a = 2, M = 1.15, \Gamma = 0.2$ using HPM

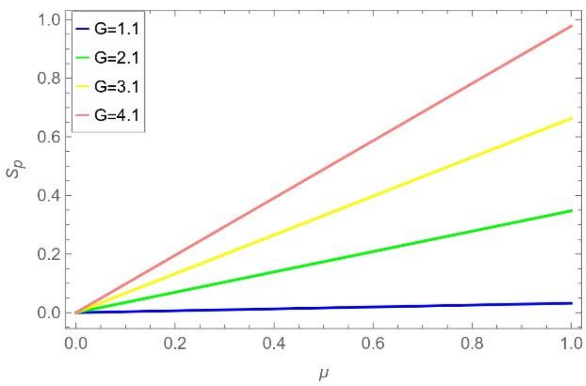

Fig. 20. Shear Stress for $\gamma = 2, M = 0.002, a = 0.1, \alpha = 165, B = 2.5, \Gamma = 0.2, A = 1$ using OHAM

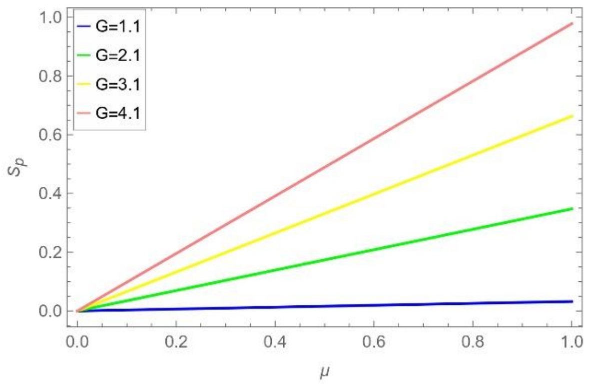

Fig. 21. Shear Stress for $\gamma = 2, M = 0.002, a = 0.1, \alpha = 165, B = 2.5, \Gamma = 0.2, A = 1$ using HPM

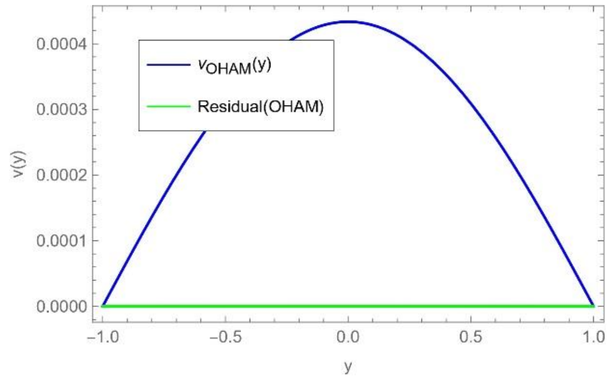

Fig. 22. Error graph of vOHAM for $\gamma = 2, M = 0.002, a = 0.1, \alpha = 165, B = 2.5, \Gamma = 0.2, A = 1$ and $G = 1$

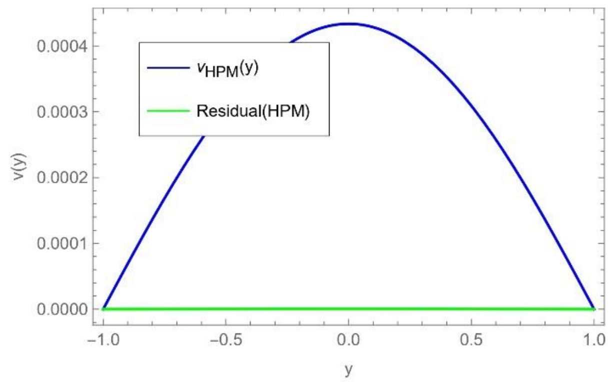

Fig. 23. Error graph of vHPM for $\gamma = 2, M = 0.002, a = 0.1, \alpha = 165, B = 2.5, \Gamma = 0.2, A = 1$ and $G = 1$

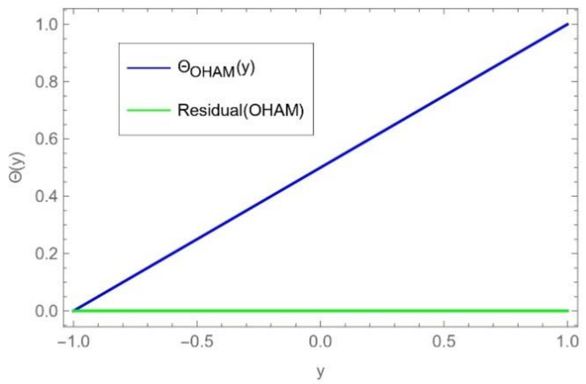

Fig. 24. Error graph of ΘOHAM for $\gamma = 2, M = 0.002, a = 0.1, \alpha = 165, B = 2.5, \Gamma = 0.2, A = 1$ and $G = 1$

DOI 10.2478/ama-2024-0058

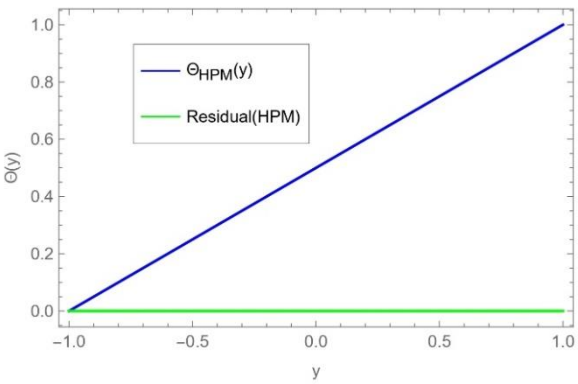

Fig. 25. Error graph of $\Theta\mathrm{HPM}$ for $\gamma = 2, \mathrm{M} = 0.002, \mathrm{a} = 0.1, \alpha = 165, \mathrm{B} = 2.5, \Gamma = 0.2, \mathrm{A} = 1$ and $\mathrm{G} = 1$

In Figures 12-19 we observed the effect of numerous parameters on temperature distribution Θ. The increase or decrease in the values of these parameters causes change in the temperature of the fluid. In Figures 14 and 15 we have seen that increase in the value of A causes increase in the temperature of the fluid. The parameter A is directly related to the temperature distribution Θ. In figures 16 and 17 a reduction in the MHD parameter enhances magnetic influence and encourages the conversion of magnetic energy into thermal energy. Due to increased heat production and decreased magnetic field resistance, this raises the fluid temperature. The influence of parameter γ on temperature distribution is visualized using graphs 18-19. Since fluid mixing is improved and internal thermal gradients are minimized as the Brinkman number rises, fluid momentum prevails over thermal conduction, resulting in a more uniform temperature distribution. This implies that viscous heating of the fluid produces more heat than heat transfer from the heated wall to the fluid. By varying the values of G, we can examine how shear stress $\mathrm{S_p}$ behaves in an inclined Poiseuille flow in Figures 20-21. The visual representation of error graphs is shown in Figures 22-25.

6. CONCLUSION

In this work, we have investigated the flow of couple stress fluids as heat was transferred between two inclined fixed plates that were parallel to each another. Analytical solutions of the problem have been obtained using HPM and OHAM. The results for velocity and temperature have been plotted graphically and discussed in detail. The important outcomes of the graphical analysis of the problem are as follows:

- MHD parameter Γ produces a Lorentz force, which suppresses turbulence and alters the velocity profile to produce a faster fluid flow. while, decreased temperature distribution in the fluid results from reduced energy loss due to magnetic drag reduction.
- Greater forced convection, thinner boundary layers, and enhanced fluid motion are all benefits of increased Brinkman number γ. Because of greater thermal mixing, increased heat transfer efficiency causes a reduction in fluid temperature distribution.

Nomenclature:

η Couple Stress Parameter
$\frac{D}{Dt}$ Material Derivative
κ Thermal Conductivity
L Gradient of Velocity
μ Viscosity Coefficient
ρ Constant Density
$\mathbf{Y}$ Velocity
$\mathbf{A}$ Rivlin Ericksen tensor
$\mathbf{B}$ Magnetic Induction
$\mathbf{C}$ Unit Tensor
$\mathbf{D}$ Current Density
$\mathbf{T}$ Cauchy Stress Tensor
Θ Temperature
c_p Specific Heat
g Body force
p Dynamic Pressure
S Extra Stress Tensor
Γ MHD Parameter
γ Brinkman number

REFERENCES

1. Stokes VK, Stokes VK. Couple stresses in fluids. Theories of Fluids with Microstructure: An Introduction. 1984;34-80.
2. Stokes, Baumann. Theories of Fluids with Microstructure. Springer Berlin Heidelberg. 1984.
3. Devakar M, Iyengar TK. Run up flow of a couple stress fluid between parallel plates. Nonlinear Analysis: Modelling and Control. 2010;15(1):29-37.
4. Devakar M, Iyengar TK. Stokes' problems for an incompressible couple stress fluid. Nonlinear Analysis: Modelling and Control. 2008;13(2):181-90.
5. Hayat T, Mustafa M, Iqbal Z, Alsaedi A. Stagnation-point flow of couple stress fluid with melting heat transfer. Applied Mathematics and Mechanics. 2013;34:167-76.
6. Akbar NS, Nadeem S. Intestinal flow of a couple stress nanofluid in arteries. IEEE transactions on nanobioscience. 2013;12(4):332-9.
7. Srinivasacharya D, Srinivasacharyulu N, Odelu O. Flow and heat transfer of couple stress fluid in a porous channel with expanding and contracting walls. International Communications in heat and mass Transfer. 2009;36(2):180-5.
8. Muthuraj R, Srinivas S, Shukla AK, Immaculate DL. Non-Darcian and thermal radiation effects on Magnetoconvection flow of Two-immiscible fluids with heat transfer. InProceedings of the 24th National and 2nd International ISHMT-ASTFE Heat and Mass Transfer Conference (IHMTC-2017) 2017. Begel House Inc..
9. Srinivasacharya D, Kaladhar K. Analytical solution of MHD free convective flow of couple stress fluid in an annulus with Hall and Ion-slip effects. Nonlinear Analysis: Modelling and Control. 2011;16(4):477-87.
10. Tsai CY, Novack M, Roffe G. Rheological and heat transfer characteristics of flowing coal-water mixtures. General Applied Science Labs. Inc. Ronkonkoma. NY (USA). 1988.
11. Yürüsoy M, Pakdemirli M. Approximate analytical solutions for the flow of a third-grade fluid in a pipe. International Journal of Non-Linear Mechanics. 2002;37(2):187-95.
12. Makinde OD. Laminar falling liquid film with variable viscosity along an inclined heated plate. Applied Mathematics and Computation. 2006;175(1):80-8.
13. Makinde OD. Thermal criticality for a reactive gravity driven thin film flow of a third-grade fluid with adiabatic free surface down an inclined plane. Applied Mathematics and Mechanics. 2009;30(3):373-80.

14. Makinde OD. Thermodynamic second law analysis for a gravity-driven variable viscosity liquid film along an inclined heated plate with convective cooling. Journal of Mechanical Science and Technology. 2010;24:899-908.
15. Qayyum M, Khan H, Rahim MT, Ullah I. Analysis of unsteady axisymmetric squeezing fluid flow with slip and no-slip boundaries using OHAM. Mathematical Problems in Engineering. 2015.
16. Ullah I, Rahim MT, Khan H, Qayyum M. Analysis of various semi-numerical schemes for magnetohydrodynamic (MHD) squeezing fluid flow in porous medium. Propulsion and Power Research. 2019;8(1):69-78.
17. Li YM, Ullah I, Ameer Ahammad N, Ullah I, Muhammad T, Asiri SA. Approximation of unsteady squeezing flow through porous space with slip effect: DJM approach. Waves in Random and Complex Media. 2022;1-5.
18. Ullah I, Rahim MT, Khan H, Qayyum M. Homotopy analysis solution for magnetohydrodynamic squeezing flow in porous medium. Advances in Mathematical Physics. 2016.
19. Qayyum M, Khan H, Rahim MT, Ullah I. Analysis of unsteady axisymmetric squeezing fluid flow with slip and no-slip boundaries using OHAM. Mathematical Problems in Engineering. 2015.
20. Ullah I, Rahim MT, Khan H. Application of Daftardar Jafari method to first grade MHD squeezing fluid flow in a porous medium with slip boundary condition. InAbstract and Applied Analysis 2014. Hindawi.
21. Abouelregal AE, Ahmad H, Yao SW, Abu-Zinadah H. Thermo-viscoelastic orthotropic constraint cylindrical cavity with variable thermal properties heated by laser pulse via the MGT thermoelasticity model. Open Physics. 2021;19(1):504-18.
22. Abouelregal AE, Ahmad H, Yao SW. Functionally graded piezoelectric medium exposed to a movable heat flow based on a heat equation with a memory-dependent derivative. Materials. 2020;13(18):3953.
23. Hussain A, Arshad M, Rehman A, Hassan A, Elagan SK, Ahmad H, Ishan A. Three-dimensional water-based magneto-hydrodynamic rotating nanofluid flow over a linear extending sheet and heat transport analysis: A numerical approach. Energies. 2021;14(16):5133.
24. Abouelregal AE, Ahmad H. A modified thermoelastic fractional heat conduction model with a single-lag and two different fractional-orders. Journal of Applied and Computational Mechanics. 2021;7(3):1676-86.
25. Anjum A, Mir NA, Farooq M, Javed M, Ahmad S, Malik MY, Alshomrani AS. Physical aspects of heat generation/absorption in the second grade fluid flow due to Riga plate: application of Cattaneo-Christov approach. Results in Physics. 2018;9:955-60.
26. Saleem S, Awais M, Nadeem S, Sandeep N, Mustafa MT. Theoretical analysis of upper-convected Maxwell fluid flow with Cattaneo–Christov heat flux model. Chinese journal of physics. 2017;55(4): 1615-1625..
27. He JH. Homotopy perturbation method for bifurcation of nonlinear problems. International Journal of Nonlinear Sciences and Numerical Simulation. 2005;6(2):207-8.
28. He JH. Approximate analytical solution for seepage flow with fractional derivatives in porous media. Computer methods in applied mechanics and engineering. 1998;167(1-2):57-68.
29. He JH. Homotopy perturbation method: a new nonlinear analytical technique. Applied Mathematics and computation. 2003;135(1):73-9.
30. He JH. Application of homotopy perturbation method to nonlinear wave equations. Chaos, Solitons & Fractals. 2005;26(3):695-700.
31. El-Shahed M. Application of He's homotopy perturbation method to Volterra's integro-differential equation. International Journal of Nonlinear Sciences and Numerical Simulation. 2005;6(2):163-8.
32. Farooq M, Rahim MT, Islam S, Siddiqui AM. Steady Poiseuille flow and heat transfer of couple stress fluids between two parallel inclined plates with variable viscosity. Journal of the Association of Arab Universities for Basic and Applied Sciences. 2013;14(1):9-18.
33. Mahian O, Mahmud S, Pop I. Analysis of first and second laws of thermodynamics between two isothermal cylinders with relative rotation in the presence of MHD flow. International Journal of Heat and Mass Transfer. 2012;55(17-18):4808-16.

Rashid Nawaz: https://orcid.org/0000-0002-4773-8446

Muhammad Farooq: https://orcid.org/0000-0003-3392-101X

Siddiq Ur Rehman: https://orcid.org/0009-0003-8596-4895

Gamal M. Ismail: https://orcid.org/0000-0002-9060-4371

Hijaz Ahmad: https://orcid.org/0000-0002-5438-5407